Title: A Retrofitting Framework for Pre-Northridge Steel Moment-Frame Buildings
Award: USGS G13AP000061, FY 2013-2014
PI: Swaminathan Krishnan (web: krishnan.caltech.edu, email: krishnan@caltech.edu)
Report Authors: Arnar Bjorn Bjornsson, John F. Hall, and Swaminathan Krishnan
Author Affiliation: California Institute of Technology
Date: Jan 31, 2015

ABSTRACT

The 1994 M_w 6.7 Northridge and 1995 M_w 6.9 Kobe earthquakes exposed an unexpected flaw in steel moment-frame buildings. The commonly utilized welded unreinforced flange, bolted web connections were observed to experience brittle fractures in a number of buildings, even at low levels of seismic demand. A majority of these buildings have not been retrofitted and may be susceptible to structural collapse in a major earthquake. A case study of retrofitting a 20-story pre-Northridge steel moment-frame building is presented. Twelve retrofit schemes are developed with varying degrees of intervention. Three retrofitting techniques are considered: upgrading the brittle beam-to-column moment resisting connections, and implementing either conventional or buckling-restrained brace elements within the existing moment-frame bays. The retrofit schemes include some that are designed to the basic safety objective of ASCE-41 Seismic Rehabilitation of Existing Buildings.

Detailed finite element models of the base line building and the retrofit schemes are constructed. The models include considerations of brittle beam-to-column moment resisting connection fractures, column splice fractures, column baseplate fractures, accidental contributions from "simple" non-moment resisting beam-to-column connections to the lateral force-resisting system, composite actions of beams with the overlying floor system, and effects of residual stresses in the steel cross-sections. In addition, foundation interaction is included through nonlinear translational springs underneath basement columns.

To investigate the effectiveness of the retrofit schemes, the building models are analyzed under ground motions from three large magnitude simulated earthquakes that cause intense shaking in the greater Los Angeles metropolitan area, and under recorded ground motions from actual earthquakes. It is found that retrofit schemes that convert the existing moment-frames into braced-frames by implementing either conventional or buckling-restrained braces are effective in limiting structural damage and mitigating structural collapse. In the three simulated earthquakes, a 20% chance of simulated collapse is realized at PGV of around 0.6 m/s for the base line model, but at PGV as large as 1.8 m/s through the retrofit schemes. However, conventional braces are observed to deteriorate rapidly. Hence, if a braced-frame that employs conventional braces survives a large earthquake, the ability of the braces to resist ground motions from aftershocks is questionable.

Introduction

Steel moment-frames are rectilinear assemblages of beams and columns with the beams rigidly connected to the columns. The frames resist lateral loads primarily by developing bending and shear forces in the frame members. During strong ground motions the frames are expected to sustain multiple cycles of significant inelastic responses. Plastic deformations are intended to primarily be confined to the ends of beams, however, some yielding may occur in columns and in beam-to-column joints (panel zones). Through these plastic deformation excursions, the frames dissipate energy imparted to the building by the ground shaking. The ability of the steel moment-frame to withstand ground shaking in a ductile manner crucially depends upon the ability of the beam-to-column connections to undergo large plasticity excursions without brittle fracture. This, unfortunately, did not turn out to be the case in the 1994 M_w 6.7 Northridge earthquake. The commonly utilized welded unreinforced flange, bolted web connections in a number of buildings experienced brittle fractures. The damaged buildings had heights in the range of one story to 26 stories, and ranged in age from under-construction to 30 years old at the time of the earthquake. They were spread over a large geographical area. Some locations experienced only moderate levels of seismic shaking [9].

The cost of potential retrofitting schemes and their impact on the architecture have not been systematically ascertained. Owners of these buildings have not only been reluctant to undertake retrofit measures, but would rather remain in the dark about the condition of these buildings, for fear of liability arising out of awareness. Furthermore, building owners have not been presented with financial incentives, such as tax breaks, to undertake retrofitting measures. Neither have the buildings been mandated to be retrofitted. As a result, many of these buildings have been left unaltered and may be susceptible to collapse in the event of a major earthquake. One may argue that because no steel moment-frame buildings collapsed in the Northridge earthquake, there is no cause for concern. However, it should be noted that the majority of the seismic energy that was released in the Northridge earthquake was directed away from urban areas into the Santa Susana mountains [39]. Moreover, larger magnitude earthquakes are expected to strike the greater Los Angeles region on well-mapped fault systems such as the San Andreas fault system as well as blind thrust faults such as the Puente Hills fault [37, 38, 36]. It is very much likely that these buildings will be subjected to far greater shaking during their lifetimes.

It is clear from the foregoing discussion that retrofit measures are necessary to reduce the collapse potential of pre-Northridge steel moment-frame buildings in the next big earthquake. These measures must realize a lower probability of collapse for the structures at a given intensity of ground shaking when compared to the existing versions. At the same time, they need to be economically feasible and, to the extent possible, must preserve the architectural integrity and funcionality of the building. In order to systematically develop a framework for retrofitting existing pre-Northridge steel moment-frame buildings, we start with a case study of a fictional 20-story building model, designed by Hall [15] according to the 1994 Uniform Building Code (UBC) provisions and studied extensively by he and his colleagues [19, 14, 16]. We develop twelve retrofit schemes with some progressively increasing degrees of intervention. Three retrofit strategies are considered in the present study: (i) upgrading the brittle beam-to-column moment resisting connections; (ii) adding conventional braces; and (iii) adding buckling-restrained braces. The retrofit schemes that involve addition of braces are designed to the basic safety objective (BSO) of ASCE-41 Seismic Rehabilitation of Existing Buildings [1].

To investigate the effectiveness of the retrofit schemes, detailed finite element models of the base line building and the retrofit schemes are constructed in STEEL, a nonlinear structural analyses program for steel frames developed at Caltech (also referred to as FRAME-2D). These models are analyzed under ground motions from three large simulated earthquake scenarios in the greater Los Angeles metropolitan area, as well as under recorded ground motions from actual earthquakes. The earthquake records are used to perform incremental dynamic analysis (IDA) of the building models. The improvement in the performance of the retrofit schemes over the base line model is quantified, and the better performing retrofit schemes are identified. Such analyses on several index buildings will provide a clear picture of the degree of retrofitting required to gain marginal reductions in the collapse potential of this class of buildings.

Building Models

Baseline Model

The base line model considered in this study is a fictional twenty-story "pre-Northridge" steel moment-frame building developed by Hall [15] and is designed to conform to the 1994 Uniform Building Code. The height of the building (above ground) is 77.9 m (255′-6″) with a typical story height of 3.8 m (12′-6″) and a taller first story at 5.5 m (18′-0″). The building has a single basement story with the same height as the first story. An isometric view of the building is shown in Fig. 1. The typical floor plan showing the arrangement of moment-frame bays is presented in Fig. 2.

Computer analyses are carried out using a 2-D analysis program developed at Caltech called STEEL (also refferred to as FRAME-2D). Several studies have been conducted to validate the program. Challa and Hall [4] showed that the behavior of a panel zone element which is used to model "joints" in STEEL agrees well with experimental data from a moment-frame subassembly test. Hall et al. [18] demonstrated a good agreement with experimental data of a cantilever beam and a slender brace element under cyclic loading. Krishnan [21, 25, 26, 22, 23, 3] extended the planar program into three dimensions and showed that both programs give similar

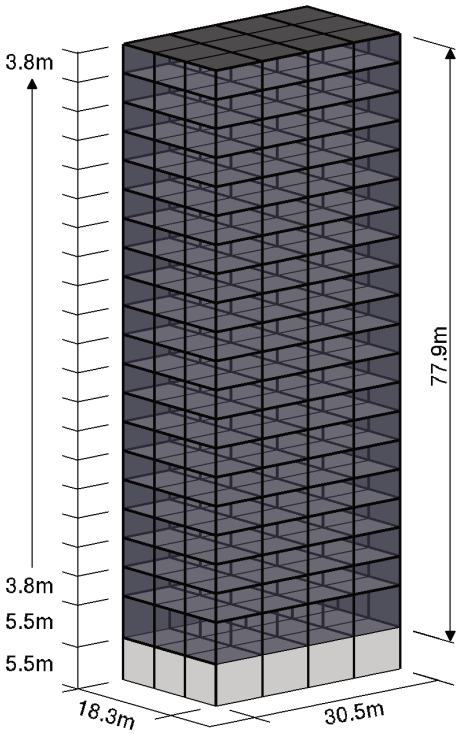

Figure 1: Isometric view of the building under study.

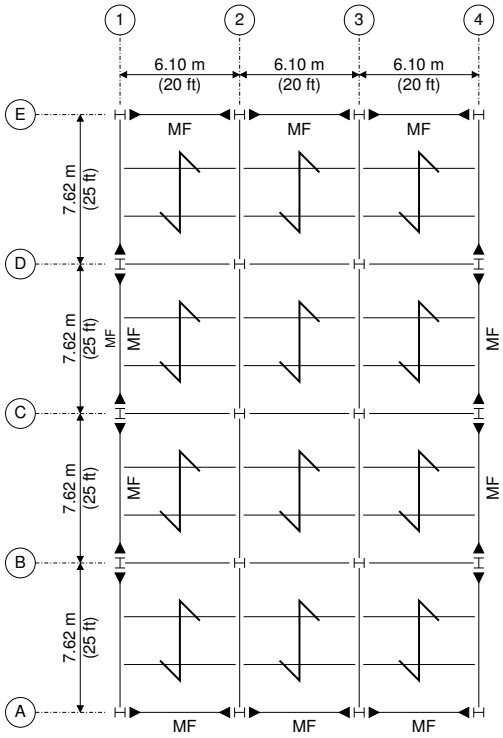

Figure 2: Typical floor plan of the building under study. Moment-resisting beam-to-column connections are indicated by solid black triangles.

results for a two dimensional moment-frame configuration, as well as good agreement with experimental data. In the present study we demonstrate further the ability of the program to model hysteretic buckling, postbuckling and tension yield of conventional brace elements. We also demonstrate the ability of the program to model cyclic loading of buckling-restrained brace elements. Sample cyclic brace responses from the exercises towards validation of the modeling of conventional braces and buckling-restrained braces are shown in Fig. 3.

Since the earthquake response of the narrow dimension of the building is of most interest, designs were carried out in this direction only. Similarly, analysis included in this study is only of the narrow dimension. Details of the design is given in [15]. Efforts are made to make the building models as realistic as possible while keeping them computationally efficient. The models include considerations of brittle beam-to-column moment resisting connection fractures, column splice fractures, column base-plate fractures, accidental contributions from "simple" non-moment resisting beam-to-column connections to the lateral force-resisting system, composite actions of beams with the overlying floor system, and effects of residual stresses in the steel cross-sections. In addition, foundation interaction is included through nonlinear (elastic-perfectly plastic) translational springs underneath basement columns. To address uncertainties associated with the modeling of the foundations, "soft" (and weak), "stiff" (and strong), as well as "expected" foundation spring stiffnesses and capacities are applied. The elastic undamped first-mode periods of the base line model for the "soft", "expected", and "stiff" realizations of the foundation interactions are 3.63 s, 3.31 s, and 3.13 s, respectively. The seismic mass is computed using full dead load and 30% of the floor live load for the vertical degrees of freedom, but using the full dead load and 20% of the floor live load for the horizontal degrees of freedom. Viscous damping is taken as a small amount (0.5%) of stiffness proportional damping at the fundamental mode plus a larger amount of nonlinear (elastic-perfectly plastic) inter-story damping. In this way, unrealistically large damping forces encountered in the use of Rayleigh damping, as demonstrated by Hall [17], are avoided.

The analysis commences with the application of the gravity loads followed by the earthquake ground

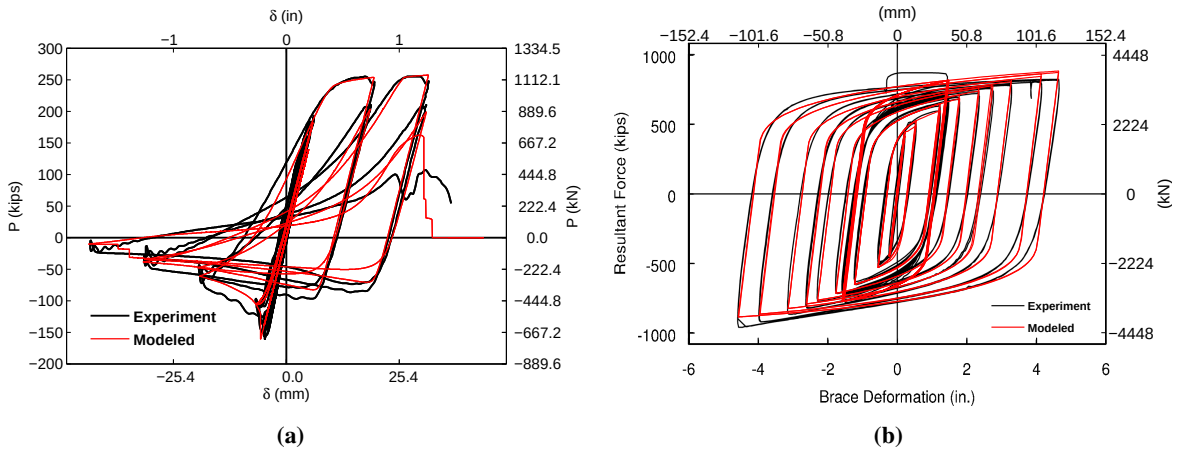

Figure 3: Measured and modeled brace axial displacement versus axial force responses of specimen (a) a conventional brace specimen (HSS1-3) from the Fell et al. testing program [6, 7] and (b) a buckling-restrained brace specimen (1G) from the Newell et al. testing program [33].

acceleration. The Constant Average Acceleration method (Newmark's method with $\gamma = 0.50$ and $\beta = 0.25$) is used for time integration. Model coordinates are updated during each iteration of a single time step and the dynamic equations of equilibrium are solved in the deformed configuration. This automatically accounts for local $P - \Delta$ effects such as element buckling as well as global $P - \Delta$ effects. The reader is directed to [2] for a more comprehensive description of the building models and the features of the analysis program

Retrofit Schemes

In the present study, three retrofitting strategies are considered: upgrading the brittle beam-to-column moment resisting connections, and adding either conventional or buckling-restrained brace elements to the existing moment-frame bays. Conventional braces refer to brace elements made of structural steel sections that buckle laterally if loaded in compression beyond their critical buckling strength. The lateral buckling mechanism leads to concentration of strains and often local buckling of the cross-section at mid-span of the element. The local buckling of the cross-section further localizes strains, which leads to severing of the cross-section and rapid deterioration of the element [6, 7]. As the name suggests, buckling-restrained braces have been developed to prevent the lateral buckling of conventional braces through lateral confinement by an unbonded enclosure. They are generally composed of a core structural steel section that has a reduced cross-sectional area over a central portion of the element. The central portion is restrained from lateral and local buckling by an enclosure (e.g., a concrete-filled tube). Debonding material is painted on the core steel-section such that it may compress and elongate independent of the enclosure. The core may yield in compression and tension alike resulting in very stable, almost symmetric hysteresis loops.

Adding brace elements to the structural system stiffens it significantly, generally shifting the dynamic character of the structure to a more energetic regime of earthquake ground motions, which results in greater forces. Hence, when brace elements are introduced, columns (and foundations) may need to be strengthened as well. In this study, strengthening of columns is assumed to be achieved by welding cover plates to the flanges.

Because comprehensive retrofit schemes can be very expensive, it is of interest to quantify the improvement in performance through partial retrofitting. With this in mind, we developed twelve retrofit schemes with some progressively increasing degrees of intervention. Six retrofit schemes are obtained by upgrading the brittle beam-to-column moment resisting connections in one, two or all three of the moment-frame bays, over half the height of the building or over the full height. We will refer to these retrofit schemes by the acronym "RMF". Two of the remaining six retrofit schemes consist of variations of addition of conventional brace elements in an inverted-V (or chevron) arrangement over the full height of the building (retrofit schemes RBR-1 and RBR-2).

A third retrofit scheme is a "partial" retrofit scheme that consists of adding conventional brace elements to the lower half of the building (retrofit scheme RBR-3). The last three schemes are obtained by replacing the conventional brace elements with buckling-restrained braces in RBR-1, RBR-2, and RBR-3. These schemes will be referred to by acronyms RBRB-1, RBRB-2, and RBRB-3, respectively. A schematic overview of the retrofit schemes considered in this study is shown in Fig. 4. The first mode natural periods assuming the "expected" realization of the foundation springs are presented in the figure as well.

The upgrade of the moment-frame connections is achieved computationally by eliminating the connection fracture susceptibility, i.e., beams are assumed to be capable of forming stable fully plasticized hinges near column faces. In the braced retrofit schemes, the moment-frame connections are assumed to have the same brittle, pre-Northridge properties. In reality, some strengthening of the connections can be expected through the addition of the gusset plates, which the brace elements are attached to. Where cover plates have been added to strengthen columns, it is assumed that these plates are able to prevent fractures in column splices and base plates. Elsewhere, column splices and base plates are not reinforced. For the braced schemes, the sizes of braces are determined through seismic design conforming to the basic safety objective (BSO) of ASCE-41 Rehabilitation of Existing Buildings [1]. The details of the designs are given in [2].

To quantify the strength of the building models, push-over analyses are performed using a similar procedure as described by Hall [15]. In these analyses, the building models are subjected to horizontal ground acceleration that increases linearly at a rate of 0.3 g per minute, and the building responses are computed dynamically. The building models are identical to those used in the earthquake analyses except that the masses of the horizontal degrees of freedom, totaling the seismic mass of the baseline model W_{BLM}/g, are redistributed according to the following equations:

$$w_i^p = C_i^p \frac{W_{BLM}}{g}, \quad C_i^p = \frac{w_i^{BLM} h_i}{\sum_{k=1}^{n} w_k^{BLM} h_k}$$

where w_i^{BLM} is the actual floor mass of the i^{th} floor of the base line model, w_i^p is the floor mass of the i^{th} floor used in the push-over analyses, h_i is the elevation (from ground level) of the i^{th} floor, and n is the number of floors above ground. The masses corresponding to the vertical degrees of freedom are omitted in the push-over analyses.

Results are presented in Figs. 5 and 6. The vertical axis is the building base shear normalized by the seismic design weight of the base line model W_{BLM}. The base shear is calculated by summing the horizontal reactions at the foundation. The horizontal axis is the building overall drift ratio, which refers to the horizontal roof displacement relative to the displacement at ground level normalized by the height of the building above ground. Push-over curves are presented for three analysis runs per building model. The three instances represent different realizations of the probability distributions describing the strengths of the beam-to-column moment resisting connections, column splices, and column base plates. Push-over curves for the base line model are also shown for comparison.

The curves are linear up to a yield or fracture point of the building model. Beyond this, the models either show some strain hardening that is followed by strength degrading behavior, or directly show a strength degrading behavior. Some curves show a drop to zero base shear and are indicative of failure mechanisms that include the first few stories. Other curves show a more moderate drop in base shear and are indicative of failure mechanisms higher up in the building models. These curves suggest that estimating the global ductility of the building models based on push-over curves can be misleading. Since the push-over analyses are performed dynamically, stiffness changes that result from yielding of structural elements and, especially, fracturing of connections cause vibrations. The resulting vibrational oscillations are apparent in the figures.

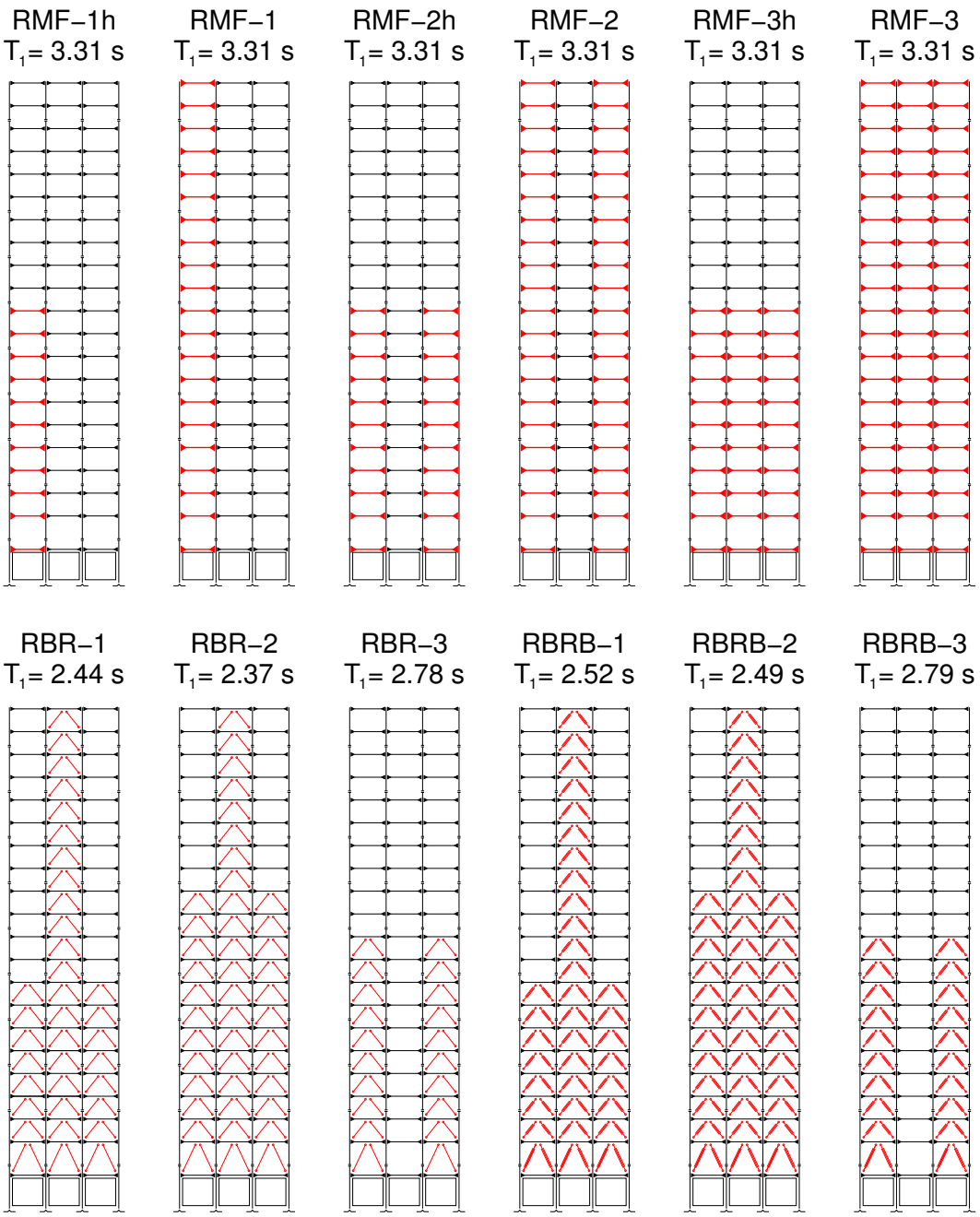

Figure 4: A schematic overview of the retrofit schemes considered in this study and associated first mode natural periods. RMF refers to retrofit schemes upgraded moment-resisting beam-to-column connections, RBR refers to retrofit schemes with added conventional braces, and RBRB refers to retrofit schemes with added buckling-restrained braces. The original pre-Northridge beam-to-column moment resisting connections are shown in black whereas the upgraded connections are shown as enlarged red triangles. The affected beams in the RMF schemes and the added braces in the RBR and BRBF schemes are shown in red as well.

Ground Motions

The greater Los Angeles metropolitan area, which is the geographic focus of this study, is seismically a highly active region. A complex network of faults surrounds, cuts through, and is buried underneath the urban area. Some faults have surface expressions and are well mapped, such as the San Andreas, the Santa Monica-Hollywood-Raymond, and Newport-Inglewood faults. Other, so-called blind-thrust, faults are buried underneath the earth's surface. These include the Puente Hills fault system that lies underneath downtown Los Angeles and the

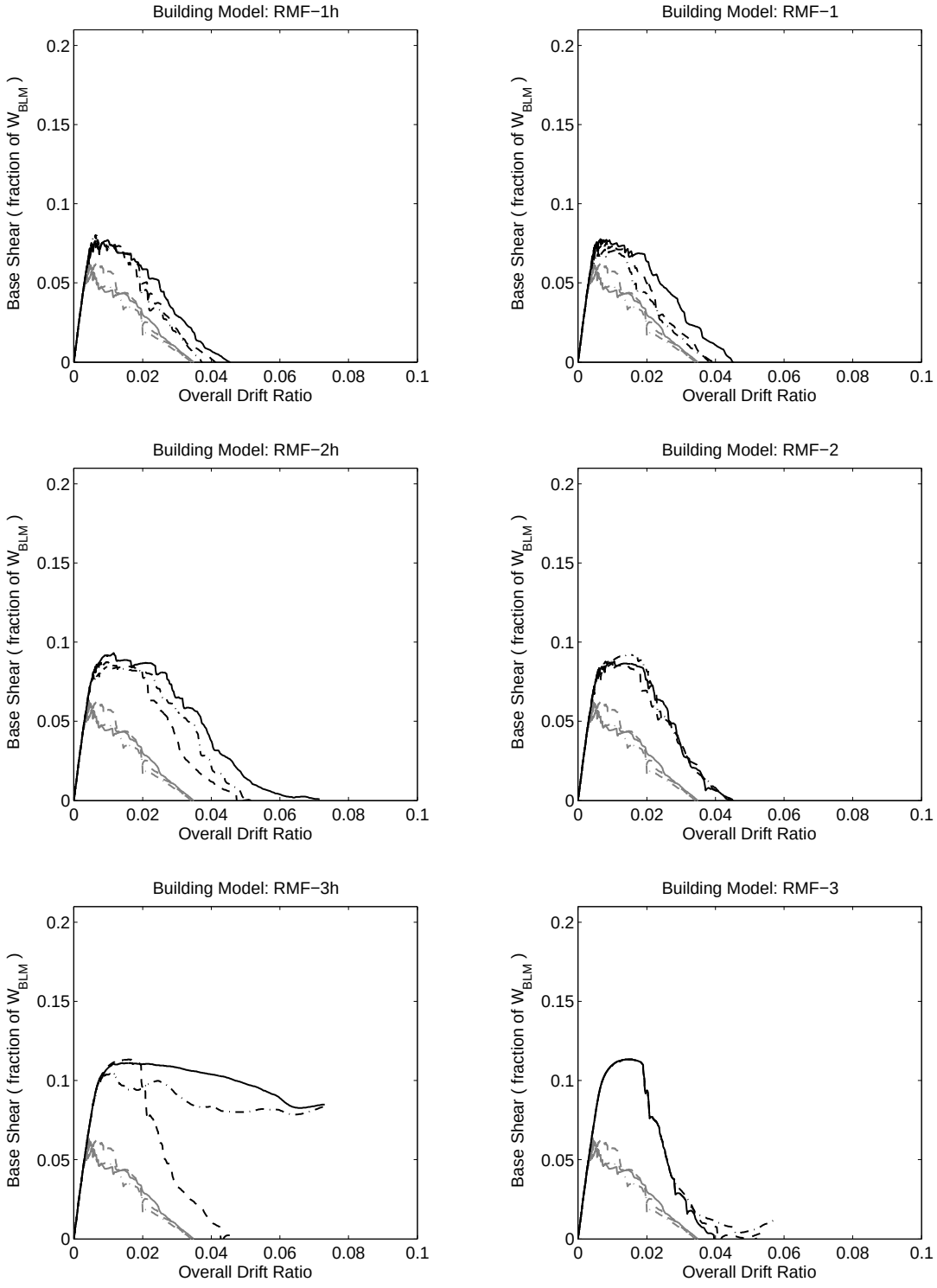

Figure 5: Push-over curves for the retrofit schemes with upgraded beam-to-column connections (black curves), and the base line model (gray curves). Three curves are shown for each building model corresponding to three different realizations of the probability distributions describing the strengths of the connections, column splices, and column base plates.

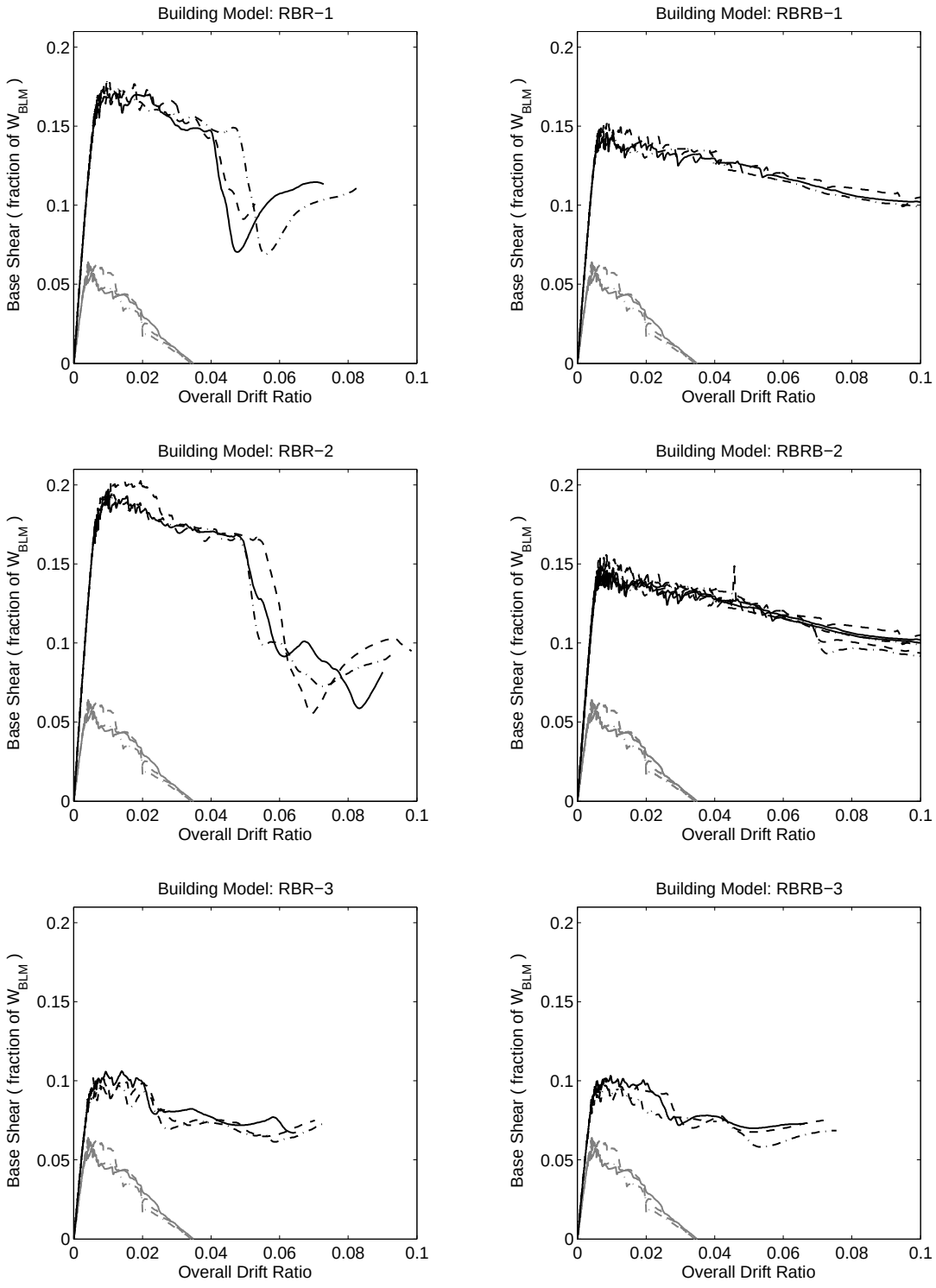

Figure 6: Push-over curves for the retrofit schemes with added conventional or buckling-restrained braces (black curves) and the base line model (gray curves). Three curves are shown for each building model corresponding to three different realizations of the probability distributions describing the strengths of the connections, column splices, and column base plates.

Northridge fault that ruptured on January 17 1994 and caused 57 deaths and economic losses in excess of $40 billion [5, 35]. The San Andreas fault has the potential of producing large ($M_w \sim 8$) earthquakes, typically every 200-300 years [37, 38]. Blind-thrust faults have the potential for more moderate ($M_w \sim 7$) earthquakes [36], but their proximity to heavily urbanized areas render them a major threat as well.

In this study we use simulated 3-component ground motions from three hypothetical earthquake scenarios that cause strong shaking in the Los Angeles metropolitan area: motions at 636 sites from a M_w 7.9 1857-like San Andreas fault earthquake produced by Krishnan et al. [28, 29, 24], motions at 784 sites from the M_w 7.8 ShakeOut scenario earthquake on the San Andreas fault produced by Graves et al. [12, 11], and motions at 587 sites from a simulated M_w 7.2 Puente Hills earthquake produced by Graves and Somerville [10, 13]. The two horizontal components from these 2087 sets of synthetic ground motions are supplemented with 20 recorded ground motion time histories from 11 past earthquakes that are scaled using 8 factors.

All the synthetic ground motions from the simulated scenario earthquakes are comprised of three component time-histories: an east-west (EW) component, a north-south (NS) component, and a vertical component. The recorded ground motions from past earthquakes are also comprised of three component time-histories, except that one horizontal component is normal to the fault rupture (fault-normal), the horizontal component is parallel to the fault rupture (fault-parallel), and a vertical component. The vertical component in the Superstition Hills earthquake record is missing, however. The planar models of the buildings are subjected to both EW and NS components of the synthetic ground motion histories. The recorded ground motion histories from past earthquakes are used to perform incremental dynamic analysis (IDA) of the building models. For this, the fault-normal and vertical components (if available) are scaled by factors ranging from 0.6 to 2.0 with increments of 0.2 and applied to the models.

Fig. 7 shows maps of the greater Los Angeles metropolitan area with the rupture extents of the three scenario earthquakes overlaid. Also shown are the locations of the sites where ground motion time histories are generated and the building models are hypothetically located. Maps of EW and NS direction peak ground velocities (PGV) realized in the simulated earthquake scenarios are shown in Fig. 8. The list of recorded ground motion time histories from past earthquakes are given in Tab. 1. The total number of simulations carried out for each building model, for each of the three foundation realizations ("stiff", "expected", and "soft"), is 4174.

Results

Quantifying Structural Performance

All thirteen building models are analyzed for the ground motions described in the previous section. Simulated building performance is classified under four performance categories: "immediate occupancy", "repairable", "unrepairable", and "collapse". The distinction between the performance categories is drawn from simulated residual inter-story drift ratio (IDR), residual building overall drift ratio (ODR), and residual foundation rotation angle. Inter-story drift ratio refers to the relative horizontal displacement of two adjacent floors normalized by the height of the story bounded by these floors. Building overall drift ratio refers to the horizontal roof displacement relative to the ground level normalized by the height of the building above ground. Foundation rotation angle is measured as the angle made by the basement level walls and the vertical axis of the building. The concrete walls at the basement level are rigid in comparison to the upper structure and the foundation springs. As a result, they primarily rotate as a rigid body as opposed to deforming in shear. Inter-story drift ratio and building overall drift ratio are corrected for floor incline. Inclination at floor levels can result from either rotation of the foundation or accumulated lengthening/shortening of columns in tension/compression. "Immediate occupancy" performance category is defined in FEMA 356 [8] as building performance where residual drift is negligible and the structure retains its original strength and stiffness. In the present work, "immediate occupancy" category is assumed if residual inter-story drift and residual foundation rotation angle is less than $\frac{1}{2000}$.

The next concern is whether the simulated building responses would indicate structural damage beyond economical repair. Iwata et al. [20] analyzed twelve steel frame buildings that suffered damage in the 1995

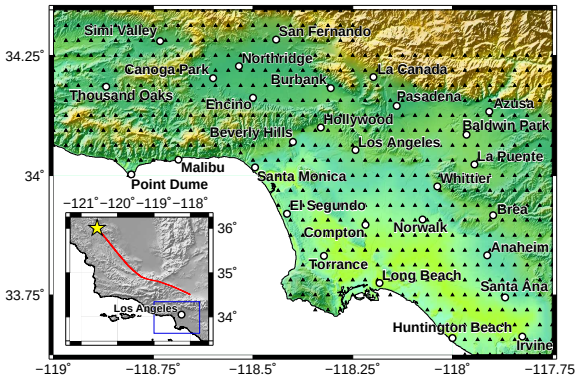

(a)

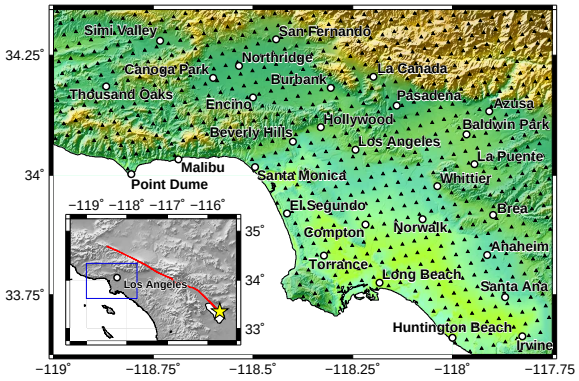

(b)

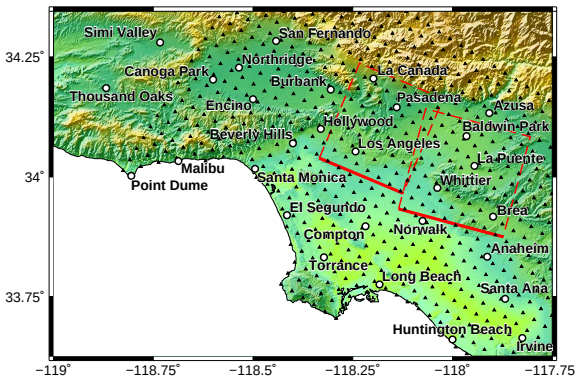

(c)

Figure 7: Geographic scope of the scenario earthquake simulations: (a) the 1857-like San Andreas fault earthquake, (b) the ShakeOut scenario earthquake on the San Andreas fault, and (c) the scenario earthquake on the Puente Hills fault system. Black triangles represent the sites where ground motion time histories are generated and the building models are analyzed. The color scheme reflects topography with green representing low elevation and yellow representing high elevations. In the insets on the maps for the 1857-like and ShakeOut scenario San Andreas fault earthquakes the red line shows the surface trace of the hypothetical rupture. The nucleation point of the rupture is indicated by a yellow star. The extent of the greater Los Angeles metropolitan region, which is the geographic focus of this study, is indicated by a blue rectangle. On the map for the earthquake scenario on the Puente Hills fault system the surface projection of the rupture is shown with red rectangles.

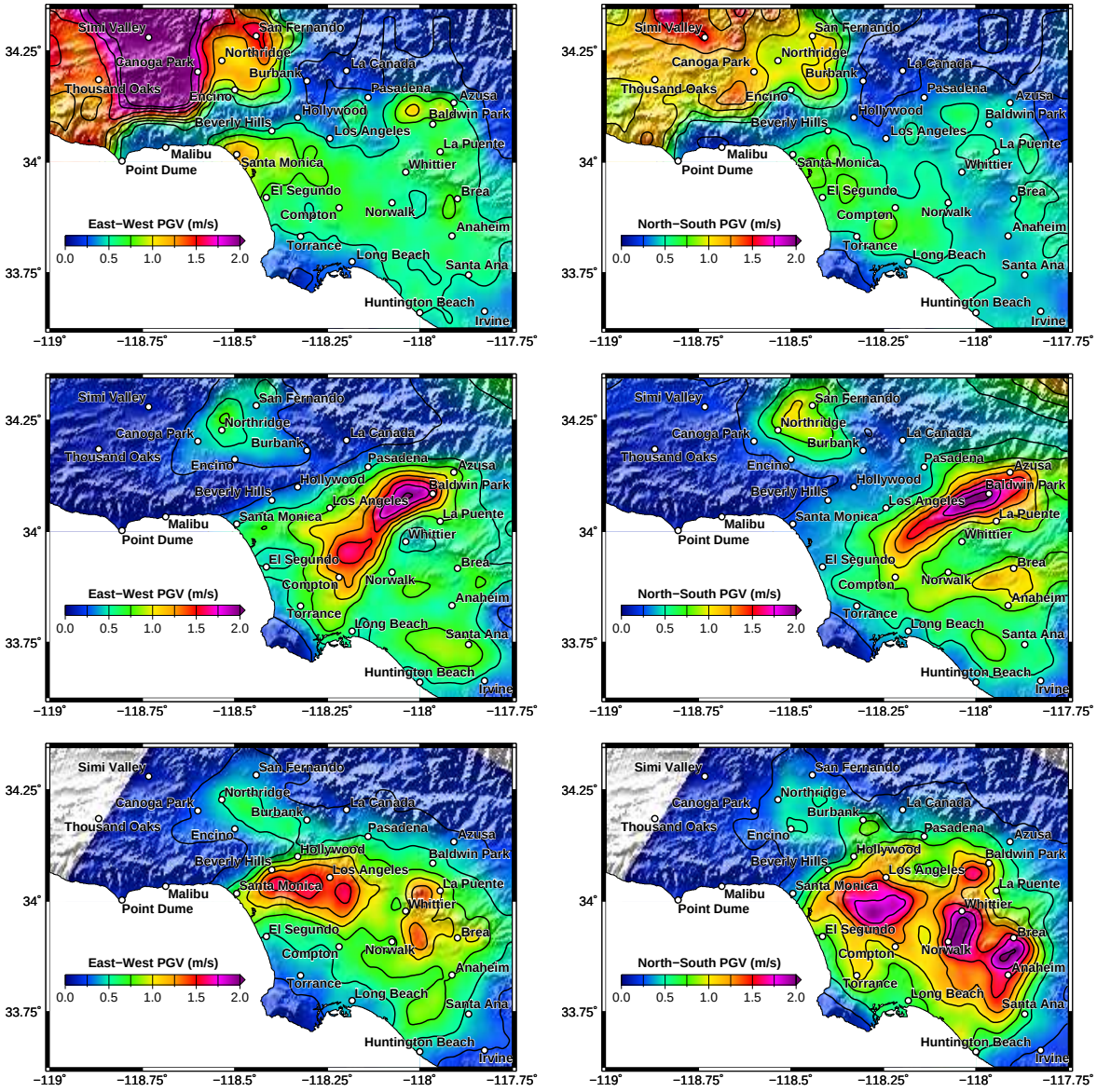

Figure 8: Peak ground velocities (PGV) realized in the greater Los Angeles metropolitan area for the east-west and north-south directions in (a)-(b) the 1857-like San Andreas fault earthquake, (c)-(d) the ShakeOut scenario earthquake on the San Andreas fault, and (e)-(f) the scenario earthquake on the Puente Hills fault system.

Table 1: List of the ground motion records from past earthquakes used in the incremental dynamic analysis of the building models.

Event	**Location**	**Year**	**Moment Magnitude**	**Station/Record**	**PGV*** **(m/s)**
Cape Mendocino	CA, USA	1992	7.2	Petrolia	1.33
Chi-Chi	Taiwan	1999	7.6	CWBC101 CWBT063 CWBT120 TCU052 TCU068	1.07 0.83 0.62 1.83 2.80
Denali	AK, USA	2002	7.9	Pump Station #10	1.09
Imperial Valley	CA, USA	1979	6.5	El Centro Array #6 El Centro Array #7 Meloland Overpass	1.13 1.13 0.95
Kobe	Japan	1995	6.9	JMA Takatori	1.07 1.54
Landers	CA, USA	1992	7.3	Lucern Valley	1.47
Loma Prieta	CA, USA	1989	6.9	Lexington Dam Los Gatos Presentation Center	1.19 1.05
Northridge	CA, USA	1994	6.7	Rinaldi Sylmar	1.63 1.32
San Fernando	CA, USA	1971	6.6	Pacoima Dam	1.15
Superstition Hills	CA, USA	1987	6.7	Superstition Mountain	1.12
Tabas (Iran)	Iran	1978	7.4	Tabas	1.28

* Fault-normal component.

Kobe earthquake in Japan and established limits on residual deformation beyond which a building would not be repaired but demolished. In that study two sets of "repairability limits" are presented: one based on whether rehabilitation could be achieved without extensive straightening repair or large-scale strengthening (if residual inter-story drift ratio exceeds $\frac{1}{71}$, or if residual overall building drift exceeds $\frac{1}{110}$), and the second based on direct and indirect repair cost to the building owner (if residual inter-story drift ratio exceeds $\frac{1}{90}$, or if residual overall building drift exceeds $\frac{1}{200}$). McCormick et al. [31] performed a review of previous research in Japan on psychological and physiological effects of residual drifts on occupants and verified these against an occupied 40-year building at Kyoto University in Japan. They concluded that incline of floors or tilt of vertical elements of $\frac{1}{200}$ are generally perceivable by occupants, and occupants of a building experience dizziness and nausea as the incline or tilt approaches $\frac{1}{100}$.

Here, a building model is deemed "unrepairable" if the residual inter-story drift ratio exceeds $\frac{1}{71}$, or if the residual overall building drift exceeds $\frac{1}{110}$, or if the foundation residual rotation angle exceeds $\frac{1}{200}$. A building model is assumed "repairable" if residual deformations are in between "immediate occupancy" and "unrepairable". Finally, "collapse" is defined as the complete loss of the lateral force-resisiting system. The performance categories are summarized in Tab. 2. This grading scheme is similar to the methodology presented by Olsen et al. [34].

Table 2: Performance categories used to classify simulated model performance, and the associated limits on selected model response parameters.

Performance Category	Residual IDR Limit	Residual ODR Limit	Residual Foundation Tilt Limit
Immediate Occcupancy	$\frac{1}{2000}$	N/A	$\frac{1}{2000}$
Repairable	$\frac{1}{71}$	$\frac{1}{110}$	$\frac{1}{200}$
Unrepairable			
Collapse	Complete loss of the lateral force-resisting system.		

Key Findings

The number of simulations that resulted in "repairable", "unrepairable", and "collapse" performance are summarized for all building models in Fig. 9. Building fragility (probability of the buildings becoming unrepairable or collapsing following an earthquake as a function of ground motion intensity at the site) curves are constructed using the ground motion data from the three scenario earthquakes and the corresponding structural response. The "unrepairable" and the "collapse" fragility curves for soft, expected, and stiff foundation models are presented in Figs. 10 and 11, respectively. These plots are constructed by sorting the data into bins based on horizontal peak ground velocities. For each bin, the fraction of the simulations that exceed a particular performance category is calculated. Then, a cumulative log-normal distribution function is fitted to the data by using the method of least squares. The data from the incremental dynamic analyses using recorded ground motions from actual earthquakes is sparse, and showed a poor fit to cumulative log-normal distribution functions and was precluded when constructing the fragility curves.

The baseline model with "expected" foundations collapses in 969 (out of 4174 cases) and rendered unrepairable or worse in 1447 of the 4174 analysis cases. Retrofit schemes RBR-2, RBRB-1, and RBRB-2 achieve the greatest reduction in number of simulated collapses, with collapses occurring in only 88, 81, and 78 simulations, respectively. Retrofit scheme RBR-1 is simulated to collapse in 125 simulations. Scheme RBR-1 is observed to localize deformations in a few stories just above the 8^{th} story, or where the bracing configuration is tapered. In contrast, schemes RBR-2, RBRB-1, and RBRB-2 deform more uniformly over the height, resulting in better performance. Scheme RBR-2 has the least number of cases (354) classified as unrepairable or worse (complete loss from an economic standpoint), followed by RBR-1 with 422 cases, RBRB-1 with 485 cases, and RBRB-2 with 468 cases. It appears that braced-frames that employ buckling-restrained braces tend to have greater residual drifts. However, the buckling-restrained braces are likely to store significant residual forces, and the residual drifts may be recovered to some extent by replacing the deformed braces. Conventional brace elements are not expected to store residual forces to the same degree.

Of the retrofit schemes with upgraded beam-to-column connections (RMF schemes), scheme RMF-3 appears to perform best with collapses in 450 simulations and total loss in 780 simulations. Interestingly, scheme RMF-2h collapses in fewer simulations (393), but is totalled in greater number of simulations (854). Retrofit schemes RMF-2 and RMF-3h are simulated to collapse in 464 and 509 simulations, respectively, and totalled in 856 and 964 simulations, respectively. Because of the complex nature of building responses under strong ground motions, it is difficult to conclusively show that repairing fewer beam-to-column connections will lead to lower collapse potential than if all the connections are upgraded. For example, the 1857-like San Andreas fault earthquake ground motions and the recorded ground motions from the past earthquakes do show a greater collapse potential for RMF-2h than for RMF-3. However, ground motions from the ShakeOut and Puente Hills earthquake scenario cause greater number of collapses in the RMF-3 model than in the RMF-2h model. It appears that there is lower site-to-site variability in these two simulations and the particular features that dominate the records happen to be more detrimental to the RMF-3 model than to the RMF-2h model. So they are not secular in their influence on the two models. Having said this, upgrading more and more number of connections in a building may result in diminishing returns in terms of performance improvement.

The two retrofit schemes with added braces in the lower half of the building model leaving the upper half unaltered (schemes RBR-3 and RBRB-3) are somewhat successful in that the schemes are more effective in limiting deformations in the lower half of the building model, compared to the moment-frame half-height retrofit schemes (RMF-1h, RMF-2h, and RMF-3h), and thus reduce to a greater extent global P-delta overturning moments. However, the resulting structures are stiffer than the moment-frame configurations and consequently attract larger seismic forces, which often results in excessive drifts in the upper half. A retrofit scheme that implements brace elements in the lower half of the building model in conjunction with upgrading beam-to-column moment connections in the upper half may present some additional improvement in building performance while keeping architectural impact low. Retrofit schemes RBR-3 and RBRB-3 collapse in 571 and 491 simulations, respectively, and are totalled in 1049 and 981 simulations, respectively.

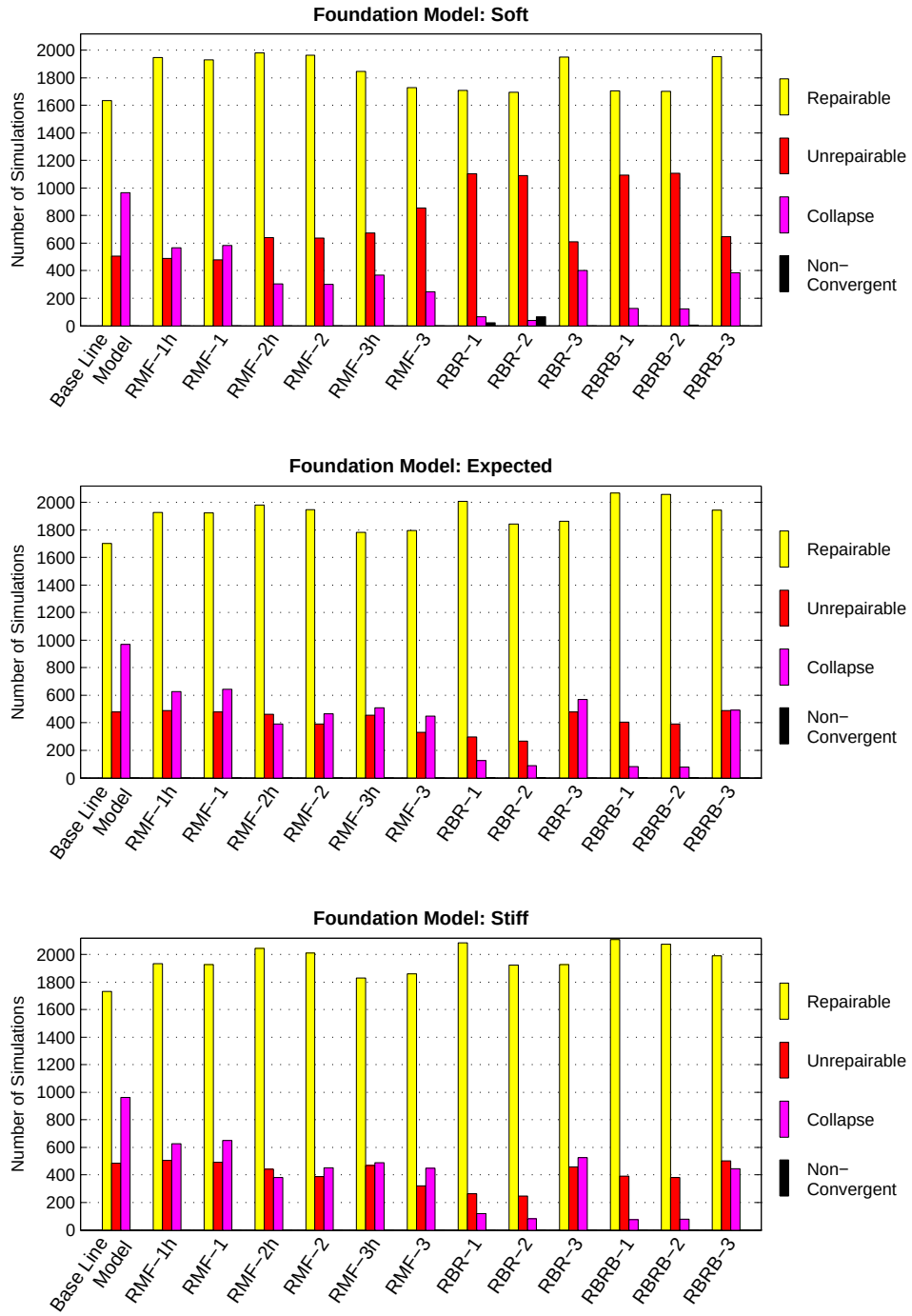

Figure 9: Bar graphs of the number of simulations that resulted in "repairable", "unrepairable", and "collapse" performance under ground motions from the three simulated scenario earthquakes as well as the scaled ground motions from past earthquakes, for the models with "soft" (top figure), "expected" (middle figure), and "stiff" (bottom figure) foundation spring stiffnesses. The total number of simulations carried out for each building model (i.e., for each of the three foundation spring stiffnesses), is 4174. Some simulations failed to converge before showing a clear sign of model collapse. These simulations are labeled as "non-convergent" and are removed from the data sets before constructing fragility curves.

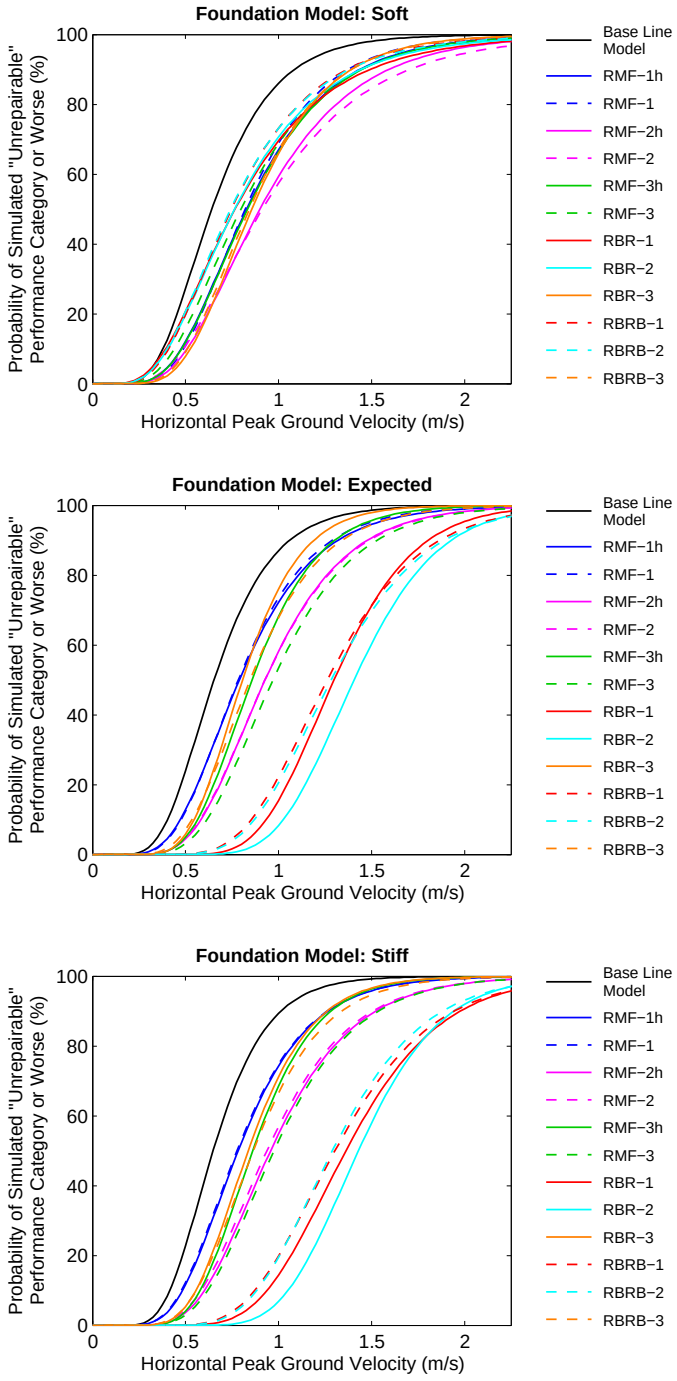

Figure 10: Fragility curves showing the probability of the building models being classified as "unrepairable" or worse given horizontal peak ground velocity in the M_w 7.9 1857-like San Andreas fault earthquake scenario, the M_w 7.8 ShakeOut scenario earthquake on the San Andreas fault, and the M_w 7.2 scenario earthquake on the Puente Hills fault system, assuming "soft" (top figure), "expected" (middle figure), and "stiff" (bottom figure) foundation spring stiffnesses.

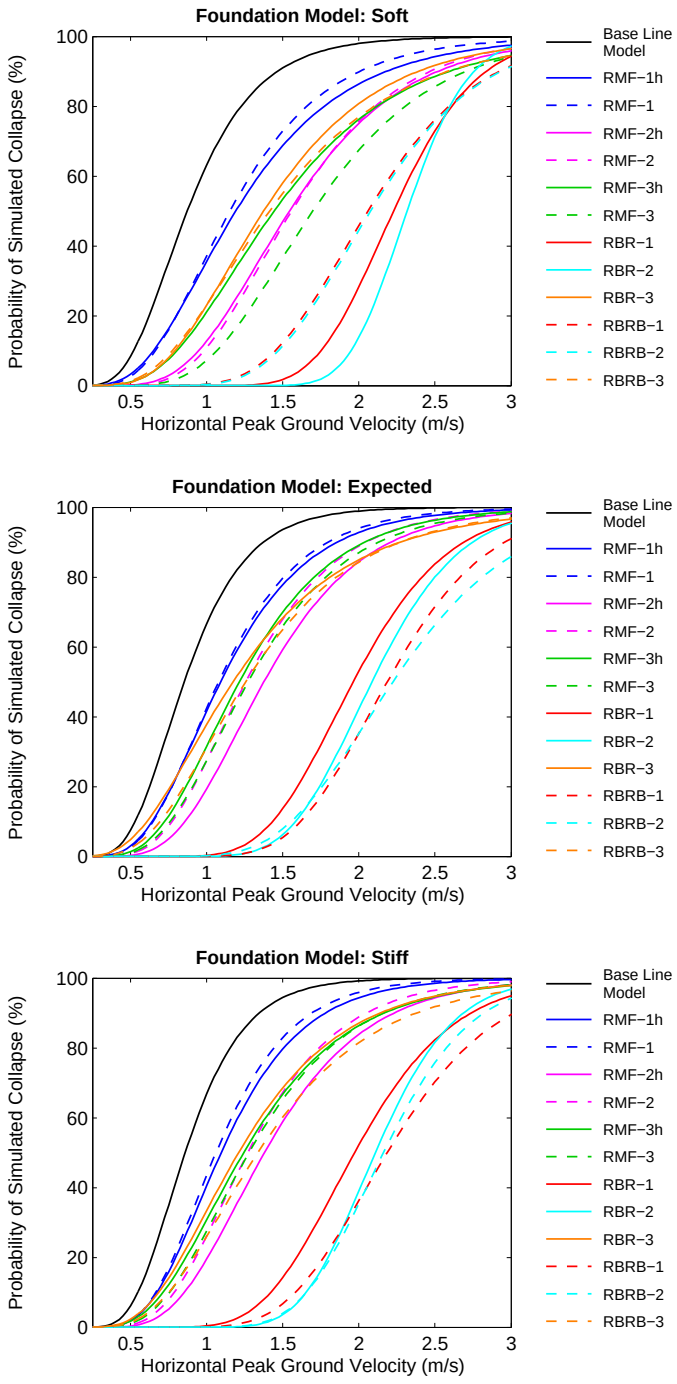

Figure 11: Fragility curves showing the probability of the building models collapsing given horizontal peak ground velocity in the M_w 7.9 1857-like San Andreas fault earthquake scenario, the M_w 7.8 ShakeOut scenario earthquake on the San Andreas fault, and the M_w 7.2 scenario earthquake on the Puente Hills fault system, assuming "soft" (top figure), "expected" (middle figure), and "stiff" (bottom figure) foundation spring stiffnesses.

From the fragility curves, the simulated building performances may be related to horizontal peak ground velocities (PGV). For instance, the PGV corresponding to a collapse probability of 20% is about 0.6 m/s for the base line model, about 1.8 m/s for retrofit schemes RBR-2, RBRB-1, and RBRB-2, about 1.6 m/s for scheme RBR-1, about 1 m/s for scheme RMF-2h, and about 0.9 m/s for schemes RMF-2, RMF-3h, and RMF-3. The horizontal PGVs corresponding to a 20% probability of "repairable" or worse performance, "unrepairable" or worse performance, and model collapse of all building models are summarized in Tab. 3.

The "expected" and "stiff" foundation models result in very similar building performances. Foundation reactions in all the building models with "stiff" foundations and all but four models with "expected" foundations are in the elastic range. Yielding of the foundation springs was observed in a few simulations of retrofit schemes RBRB-1 and RBRB-2, and a number of simulations of schemes RBR-1 and RBR-2, with residual foundation rotations up to around 1.5%. A few simulations of schemes RBR-1, RBR-2, and RBRB-2 with "soft" foundations failed to converge before showing a clear sign of collapse, which prevents a fair comparison of the building models. Nonetheless, a few interesting observations could still be made. The capacities of the foundation springs in the "soft" foundation building models were frequently exceeded. The potential for exceeding the "immediate occupancy" foundation residual rotation limit was uniform across all building models, and only modest reduction in the number of simulated cases that are totalled is observed for the retrofit schemes. It should be noted that foundation instability was not simulated and residual foundation rotations as large as 10% were observed. Under these conditions, retrofitting was much more effective in reducing the collapse potential as compared to cases with "expected" and "stiff" foundations.

Conclusions

From the analyses of the building models the following conclusions may be drawn:

(a) Pre-Northridge steel moment-frame buildings in the 20-story height can be expected to suffer severe damage and even building collapse at several locations if a major earthquake strikes the greater Los Angeles metropolitan area. Similar observations were made by Hall et al. [19, 14, 15, 16], Krishnan et al. [27, 28, 29], Muto and Krishnan [30, 32] and Olsen et al. [34]. Although other building types, such as unreinforced concrete and masonry buildings, may be in even greater risk of suffering severe structural damage or collapse, the seismic risk of pre-Northridge steel moment-frame buildings should not be neglected.

(b) Retrofit schemes that convert existing moment-frames to braced-frames by adding either conventional or buckling-restrained braces, and designed to the basic safety objective (BSO) of ASCE 41 Seismic Rehabilitation of Existing Structures [1] using a nonlinear dynamic design procedure, are effective in reducing collapse potential and avoiding unrepairable building damage of pre-Northridge steel moment-frame buildings in the 20-story range.

(c) Relying on conventional brace elements to resist seismic lateral forces is not without complications. Under strong ground motions the brace elements buckle in compression, resulting in a dramatic drop in stiffness and strength. Furthermore, the brace elements do not necessarily buckle simultaneously over the entire height of the building. Hence, the braced-frame has a tendency to develop soft and weak stories in the most stressed portion of the building. Also, during buckling a brace element experiences strain concentrations in the plastic hinge that forms at mid-span. If the excessive strains do not already cause severing of the cross-section during the buckling phase, the strain hysteresis built into the cross-section dramatically limits the ductility of the element in consequent tension cycles. In the present study conventional brace elements are observed to completely fail at inter-story drifts as low as 3%. If local buckling of the cross-sections was included in the modeling, complete element failure might be observed even sooner. So if the braced-frame survives a strong earthquake, it is questionable how effective the brace elements would be in potential aftershocks. Additionally, conventional braces are observed to experience large out-of-plane deformations during buckling, which could lead to hazards associated with falling debris.

Table 3: Horizontal peak ground velocities (m/s) at which there is a 20% probability of realizing "repairable" performance or worse, "unrepairable" performance or worse, and collapse in the building models under ground motions from the M_w 7.9 1857-like San Andreas fault earthquake, the M_w 7.8 ShakeOut scenario earthquake on the San Andreas fault, and the M_w 7.2 scenario earthquake on the Puente Hills fault system.

Building Performance:	"Repairable" or Worse			"Unrepairable" or Worse			Collapse		
Building Model: / **Foundation Model:**	"Soft"	"Expected"	"Stiff"	"Soft"	"Expected"	"Stiff"	"Soft"	"Expected"	"Stiff"
BLM[a]	0.20	0.18	0.18	0.45	0.48	0.48	0.62	0.62	0.65
RMF-1h	0.20	0.20	0.20	0.58	0.58	0.58	0.80	0.78	0.80
RMF-1	0.20	0.20	0.20	0.58	0.58	0.58	0.80	0.78	0.78
RMF-2h	0.20	0.25	0.23	0.62	0.68	0.70	1.12	1.00	1.00
RMF-2	0.20	0.25	0.23	0.60	0.68	0.68	1.15	0.90	0.93
RMF-3h	0.20	0.25	0.25	0.58	0.65	0.68	0.98	0.88	0.88
RMF-3	0.20	0.28	0.28	0.55	0.73	0.73	1.25	0.90	0.90
RBR-1	0.20[b]	0.30	0.30	0.50[b]	1.05	1.07	1.90[b]	1.60	1.60
RBR-2	0.20[b]	0.33	0.33	0.50[b]	1.15	1.18	2.08[b]	1.75	1.80
RBR-3	0.20	0.25	0.25	0.62	0.62	0.65	0.95	0.75	0.83
RBRB-1	0.20	0.30	0.28	0.50	0.98	1.00	1.62	1.80	1.78
RBRB-2	0.20[b]	0.30	0.30	0.50[b]	1.00	1.00	1.65[b]	1.75	1.83
RBRB-3	0.20	0.25	0.25	0.60	0.62	0.65	0.95	0.85	0.93

[a] Base Line Model

[b] Some simulations for retrofit schemes RBR-1, RBR-2, and RBRB-2 failed to converge before showing a clear sign of collapse, which may have an effect on these presented values.

(d) The schemes with buckling-restrained braces (BRBs) perform markedly better. Although BRBs have greater unit cost than conventional braces, using BRBs may turn out to be more economical. Adding braces to an existing moment frame building stiffens it, shifting its dynamic characteristics to a more energetic regime of the earthquake ground motion. This results in greater stiffness forces requiring column and foundation strengthening. Because conventional braces experience a dramatic drop in strength during buckling, large sections may be needed to satisfy the basic safety objective. In contrast, BRBs exhibit similar behavior in tension and compression excursions, and could be relatively smaller, imposing lower additional demands on the columns and foundations. Additionally, schemes RBR-2 and RBRB-1 (and RBRB-2) exhibit similar collapse potential. This suggests that fewer BRBs may be needed to achieve a certain level of building performance, which points to lower retrofit costs relative to conventional braces and lesser impact on the architecture.

(e) In the retrofit scheme (RBR-1) with conventional braces added in all three moment-frame bays of the bottom eight stories and in only one moment-frame bay in the upper stories, deformations were observed to localize in the region just above the eighth story, where the leaner bracing configuration begins. This deformation localization was not observed in the corresponding scheme (RBRB-1) with BRBs in the place of conventional braces.

(f) Upgrading the brittle beam-to-column connections results in some improved building performance. However, beyond a certain fraction of upgraded connections, additional connection upgrades result in diminishing returns in performance.

(g) The retrofit schemes that consider strengthening the lower half of the building by implementing brace elements while leaving the upper half unaltered (schemes RBR-3 and RBRB-3) are somewhat successful. The schemes are more effective in reducing deformations in the lower half of the building model than the half-height upgraded connection retrofit schemes. This results in lower global P-delta overturning moments. However, the resulting increase in stiffness leadng to greater seismic forces even in the upper portion of the structure diminishes this advantage. A retrofit scheme with added braces in the lower half of the building in conjunction with upgraded beam-to-column moment connections in the upper half may best balance the twin objectives of improved building performance and limited architectural impact.

(h) Three foundation types were modeled, “soft”, “expected”, and “stiff” foundations. The “expected” and “stiff” foundation models resulted in very similar building performances. Limited yielding was observed in the “expected” foundation models for some of brace retrofit schemes, but none was observed in the “stiff” foundation models. The “soft” foundation models exhibited significant yielding with residual rotations as large as 10%. But because foundation stability under such large rotations was not modeled, the collapse potential of the building models with “soft” foundations were not too different from those with “expected” and “stiff” foundations.

(i) Ground motions from all three earthquake scenarios (1857-like San Andreas earthquake, the Shakeout earthquake on the San Andreas fault, and the Puente Hills blind thrust earthquake) cause the base line model to collapse at several locations in the greater Los Angeles metropolitan area. The two San Andreas fault earthquakes produce longer duration of shaking, which proves to be a greater challenge for preventing collapse through retrofitting measures. The most destructive ground motion time histories are found in the 1857-like San Andreas fault earthquake. These time histories are of long duration with PGVs as high as 3.5 m/s at a few locations. In contrast, the largest PGVs observed in the ShakeOut scenario earthquake and the Puente Hills earthquake are around 2.5 m/s.

REFERENCES

[1] ASCE. *Seismic Rehabilitation of Existing Buildings*. American Society of Civil Engineers, USA, 2007.

[2] BJORNSSON, A. B. *A Retroffitting Framework for pre-Northridge Steel Moment-Frame Buildings*. Dissertation (Ph.D.). California Institute of Technology, Pasadena, California, 2014.

[3] BJORNSSON, A. B., AND KRISHNAN, S. A low-complexity candidate for benchmarking collapse-prediction of steel braced structures. *Special Issue on Computational Simulation in Structural Engineering, Journal of Structural Engineering 140*, 8 (2014).

[4] CHALLA, V. R. M., AND HALL, J. F. Earthquake collapse analysis of steel frames. *Earthquake Engineering and Structural Dynamics 23*, 11 (1994), 1199–1218.

[5] EGUCHI, R. T., GOLTZ, J. D., TAYLOR, C. E., CHANG, S. E., FLORES, P. J., JOHNSON, L. A., SELIGSON, H. A., AND BLAIS, N. C. Direct economic losses in the Northridge earthquake: A three-year post-event perspective. *Earthquake Spectra 14*, 2 (1998), 245–264.

[6] FELL, B. V. Large-scale testing and simulation of earthquake-induced ultra low cycle fatigue in bracing members subjected to cyclic inelastic buckling. Tech. Rep. Ph.D. Dissertation, University of California, Davis, 2008.

[7] FELL, B. V., KANVINDE, A. M., DEIERLEIN, G. G., AND MYERS, A. T. Experimental investigation of inelastic cyclic buckling and fracture of steel braces. *Journal of Structural Engineering 135*, 1 (2009), 19–22.

[8] FEMA. *Prestandard and Commentary for the Seismic Rehabilitation of Buildings*. FEMA-356. Federal Emergency Management Agency, USA, 2000.

[9] FEMA. *State of the Art Report on Connection Performance*. FEMA-355D. Federal Emergency Management Agency, USA, 2000.

[10] GRAVES, R. W. Broadband simulation for a Mw 6.7 earthquake on the Puente Hills fault. *Seismological Research Letters 76* (2005), 242.

[11] GRAVES, R. W., AAGAARD, B. T., AND HUDNUT, K. W. The ShakeOut earthquake source and ground motion simulations. *Earthquake Spectra 27*, 2 (2011).

[12] GRAVES, R. W., AAGAARD, B. T., HUDNUT, K. W., STAR, L. M., STEWART, J. P., AND JORDAN, T. H. Broadband simulations for M_w 7.8 southern San Andreas earthquakes: Ground motion sensitivity to rupture speed. *Geophysical Research Letters 35*, L22302, doi:10.1029/2008GL035750 (2008).

[13] GRAVES, R. W., AND SOMERVILLE, P. Broadband ground motion simulations for scenario ruptures of the Puente Hills fault. In *8^{th} National Conference on Earthquake Engineering, San Francisco, USA* (2006), Paper No. 1052.

[14] HALL, J. F. Parameter study of the response of moment-resisting steel frame buildings to near-source ground motions. Tech. Rep. EERL 95-08, Earthquake Engineering Research Laboratory, California Institute of Technology, Pasadena, California, 1995.

[15] HALL, J. F. Seismic response of steel frame buildings to near-source ground motions. Tech. Rep. EERL 97-05, Earthquake Engineering Research Laboratory, California Institute of Technology, Pasadena, California, 1997.

[16] HALL, J. F. Seismic response of steel frame buildings to near-source ground motions. *Earthquake Engineering and Structural Dynamics 27*, 12 (1998), 1445–1464.

[17] HALL, J. F. Problems encountered from the use (or misuse) of Rayleigh damping. *Earthquake Engineering and Structural Dynamics 35*, 5 (2006), 525–545.

[18] HALL, J. F., AND CHALLA, V. R. M. Beam-column modeling. *Journal of Engineering Mechanics 121*, 12 (1995), 1284–1291.

[19] HEATON, T. H., HALL, J. F., WALD, D. J., AND HALLING, M. W. Response of high-rise and base-isolated buildings to a hypothetical m 7.0 blind thrust earthquake. *Science 267* (1995), 206–211.

[20] IWATA, Y., SUGIMOTO, H., AND KUWAMURA, H. Reparability limit of steel structural buildings based on the actual data of Hyogoken-Nanbu earthquake. *Technical Memorandum of Public Works Research Institute 4022* (2006), 86–95.

[21] KRISHNAN, S. Three-dimensional nonlinear analysis of tall irregular steel buildings subject to strong ground motion. Tech. Rep. EERL 2003-01, Earthquake Engineering Research Laboratory, California Institute of Technology, Pasadena, California, USA, 2003.

[22] KRISHNAN, S. On the modeling of elastic and inelastic, critical- and post-buckling behavior of slender columns and bracing members. Tech. Rep. EERL 2009-03, Earthquake Engineering Research Laboratory, California Institute of Technology, Pasadena, California, USA, 2009.

[23] KRISHNAN, S. The modified elastofiber element for steel slender column and brace modeling. *Journal of Structural Engineering 136*, 11 (2010), 1350–1366.

[24] KRISHNAN, S., CASAROTTI, E., GOLTZ, J., JI, C., KOMATITSCH, D., MOURHATCH, R., MUTO, M., SHAW, J. H., TAPE, C., AND TROMP, J. Rapid estimation of damage to tall buildings using near real-time earthquake and archived structureal simulations. *Bulletin of the Seismological Society of America 102*, 6 (2012), 2646–2666.

[25] KRISHNAN, S., AND HALL, J. F. Modeling steel frame buildings in three dimensions – Part I: Panel zone and plastic hinge beam elements. *Journal of Engineering Mechanics 132*, 4 (2006), 345–358.

[26] KRISHNAN, S., AND HALL, J. F. Modeling steel frame buildings in three dimensions – Part II: Elastofiber beam element and examples. *Journal of Engineering Mechanics 132*, 4 (2006), 359–374.

[27] KRISHNAN, S., JI, C., KOMATITSCH, D., AND TROMP, J. Performance of 18-story steel moment frame buildings during a large San Andreas earthquake – a Southern California-wide end-to-end simulation. Tech. Rep. EERL 2005-01, http://caltecheerl.library.caltech.edu, Earthquake Engineering Research Laboratory, California Institute of Technology, Pasadena, California, USA, 2005.

[28] KRISHNAN, S., JI, C., KOMATITSCH, D., AND TROMP, J. Case studies of damage to tall steel moment frame buildings in southern California during large San Andreas earthquakes. *Bulletin of the Seismological Society of America 96*, 4 (2006), 1523–1537.

[29] KRISHNAN, S., JI, C., KOMATITSCH, D., AND TROMP, J. Performance of two 18-story steel moment frame buildings in southern California during two large simulated San Andreas earthquakes. *Earthquake Spectra 22*, 4 (2006), 1035–1061.

[30] KRISHNAN, S., AND MUTO, M. SHAKEOUT 2008: Tall steel moment frame building response. Tech. Rep. Technical report to the US Geological Survey, California Institute of Technology, Pasadena, California, USA, 2008.

[31] MCCORMICK, J., ABURANO, H., IKENAGA, M., AND NAKASHIMA, M. Permissible residual deformation levels for building structures considering both safety and human elements. In *Proceedings of the 14^{th} World Conference on Earthquake Engineering* (2008), pp. Paper No. 05–06–0071.

[32] MUTO, M., AND KRISHNAN, S. Hope for the best, prepare for the worst: Response of tall steel buildings to the shakeout scenario earthquake. *Earthquake Spectra 27*, 2 (2011).

[33] NEWELL, J., UANG, C., AND BENZONI, G. Subassemblage testing of CoreBrace buckling-restrained braces (G-series). Tech. Rep. TR-2006/01, University of California, San Diego, La Jolla, California, USA, 2006.

[34] OLSEN, A., HEATON, T., AND HALL, J. Characterizing ground motions that collapse steel, moment-resisting frames or make them unrepairable. *Earthquake Spectra* (2013), in press.

[35] PETAK, W. J., AND ELAHI, S. The Northridge earthquake, USA, and its economic and social impact. In *EuroConference on Global Change and Catastrophe Risk Management, Earthquake Risks in Europe, IIASA, Laxenburg, Austria* (2000).

[36] SHAW, J. H., AND SUPPE, J. Earthquake hazards of active blind-thrust faults under the central Los Angeles basin. *Journal of Geophysical Research 101*, B4 (1996), 8623–8642.

[37] SIEH, K. E. A study of late Holocene displacement history along the south-central reach of the San Andreas fault. Tech. Rep. Ph.D. Dissertation, Stanford University, California, USA, 1977.

[38] SIEH, K. E. Pre-historic large earthquakes produced by slip on the San Andreas fault at Pallett creek, California. *Journal of Geophysical Research 83* (1978), 3907–3939.

[39] WALD, D. J., HEATON, T. H., AND HUDNUT, K. W. A dislocation model of the 1994 Northridge, California, earthquake determined from strong-motion, GPS, and leveling-line data. *Bulletin of the Seismological Society of America 86* (1996), S49–S70.